C-Band Radiometric Response to Rainfall Events in the Subtropical Chaco Forest

F. Grings, V. Douna, V. Barraza, M. Salvia, H. Karszenbaum, N. I. Gasparri, P. Ferrazzoli, and R. Rahmoune

***Abstract*—In this letter, multitemporal signatures collected by Advanced Microwave Scanning Radiometer (AMSR-E) over the dry forest of Chaco, located in North Argentina, are analyzed. The forest has a biomass of about 100 t/ha and a woody volume of about 120 m^3/ha. A clear increase of polarization index at C-band is observed after intense rain events in two different locations. Simulations of a discrete model attribute this effect to variations of soil moisture and predict an effect comparable with the measured one. Results indicate that there is a potential to monitor soil moisture variations below dry forests with moderate biomass, also in view of the forthcoming availability of L-band data.**

***Index Terms*—Forests, microwave radiometry, modeling, soil moisture.**

I. Introduction

MONITORING soil moisture at large scale is a fundamental objective of microwave satellite missions. Multifrequency radiometric systems, such as Advanced Microwave Scanning Radiometer (AMSR-E) [1], have been operating at C-band (6.9 GHz) and higher frequencies for several years with various applications, including soil moisture monitoring [2]. However, the specific properties of some dry forests, covering extended areas of the world, should be considered. In these areas, the soil is generally dry for long intervals of time, and the wood volume per unit area is relatively low. These conditions can make variations in soil properties detectable, even at AMSR-E operation frequencies.

On the other hand, monitoring soil moisture is particularly important for dry forest ecosystems, since it is the most important limiting variable for productivity [3].

The objective of this letter is to investigate the effects of strong rainfall events, which occurred in dry forests with moderate wood volumes, on AMSR-E C-band signatures. We considered two homogeneous areas within the South American Chaco forest, and we evaluated the variations of the normalized polarization difference (polarization index PI) [4]. Previous studies demonstrated that this index is sensitive to vegetation biomass, but at the lower frequencies it is also influenced by soil moisture (see, e.g. [2]).

Although these basic concepts are known, further investigations, particularly on forests, are useful for various reasons. AMSR-E signatures were scarcely exploited to detect variations of soil moisture below forest covers, since this detection can be prevented by the high canopy attenuation. However, moderately dense dry forests worth to be specifically investigated. This can be useful for the exploitation of the same AMSR-E, but also in view of current and future systems employing L band. Some experimental investigations, carried out over coniferous forests or deciduous forests in cold climates, indicate that the effects of soil moisture variations on radiometric signatures are very low, even at L-band [5], [6]. Other experiments indicate that a moderate sensitivity to variations of soil moisture exists at least at L-band [7]. Since resolute conclusions have not yet been reached, it is useful to make further investigations, covering different climatic conditions and forest environments.

In this letter, we selected an area of the Chaco Forest and considered two strong rainfall events that occurred in 2006 and 2007. Rainfall data of two different stations within the selected area are available. Moderate but detectable increases of PI are observed after both rain events. We discuss possible causes of these increases, and we conclude that a sound explanation to the observations includes a change in soil properties. These considerations are confirmed by parametric simulations carried out by means of a discrete radiative transfer model.

II. Study Area

A. General Properties

In Argentina, the Chaco region includes the southernmost subtropical dry forests of America (between 22° S–32° S and 59.5° W–68° W). The Chaco Forest is a dry forest that can be considered subtropical, with a strong pattern of monsoonal seasonality occurring mainly between November and March and low annual rainfall.

The areas selected by us are located in the Semiarid Chaco subregion, in northwestern Argentina (Fig. 1). The specific study areas are in the region surrounding the two available meteorological stations, Las Lomitas and Nueva Pompeya. The climate of this region is subtropical with a dry season. The mean evapotranspiration is 15 mm h^{-1} and the mean annual precipitation is 900 mm.

We selected these areas for the following reasons: 1) the availability of daily precipitation data; 2) the existence of large

Manuscript received January 31, 2011; revised April 7, 2011 and May 24, 2011; accepted July 12, 2011. Date of publication September 15, 2011; date of current version February 8, 2012. This work was supported in part by the Agencia Nacional de Promoción Científica y Tecnológica under Project 1206 and in part by the Consejo Nacional de Investigaciones Científicas y Técnicas–Comisión Nacional de Actividades Espaciales–Ministerio de Ciencia, Tecnología e Innovación Productiva (MINCYT) under Project 13.

F. Grings, V. Douna, V. Barraza, M. Salvia, and H. Karszenbaum are with the Instituto de Astronomía y Física del Espacio (IAFE), 1428 Buenos Aires, Argentina (e-mail: verderis@iafe.uba.ar; vanedouna@gmail.com; vdbarraza@gmail.com; msalvia@iafe.uba.ar; haydeek@iafe.uba.ar).

N. I. Gasparri is with the Instituto de Ecología Regional (IER), Universidad Nacional de Tucumán, 4107 Tucumán, Argentina (e-mail: ignacio.gasparri@gmail.com).

P. Ferrazzoli and R. Rahmoune are with Tor Vergata University, Ingegneria-DISP, 00133 Rome, Italy (e-mail: ferrazzoli@disp.uniroma2.it; rahmoune@disp.uniroma2.it).

Digital Object Identifier 10.1109/LGRS.2011.2162484

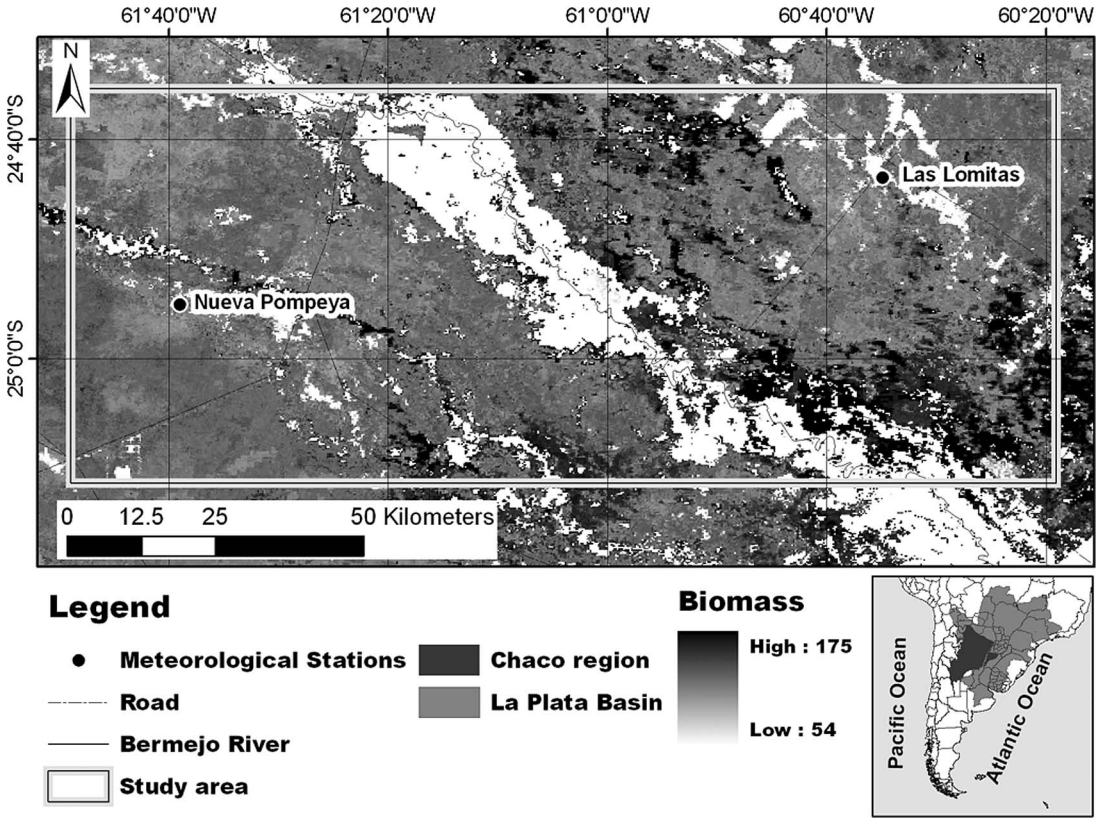

Fig. 1. Map of the study area indicating the main geographical landmarks. Superimposed is a biomass map of the area derived using optical images, ancillary data, and *in situ* measurements [10].

TABLE I
SUMMARY OF AVAILABLE MEASUREMENTS OF FOREST VARIABLES [8], [10]

Variable	Value	
Mean basal area (sum of trunk sections at 1.3 m height) [m^2/ha]	10.55	
Tree density [ha^{-1}] subdivided into classes of DBH (Diameter at Breast Height, [cm])	DBH [cm]	tree density by classes [ha^{-1}]
	5 - 10	390 ±70
	10 - 30	103 ± 37
	30 - 50	41 ± 15
	50 - 70	7 ± 4
	70 - 100	1
	> 100	0
Mean Above-Ground Biomass (Tn ha^{-1})	100 ± 12.7	

and continuous forest patches; and 3) the fact that basic forest properties of the area are routinely measured by the Unidad de Manejo del Sistema de Evaluación Forestal [8], [9]. The natural vegetation is a subtropical dry forest dominated by *Schinopsis lorentzii* (Griseb.) Engl.; *Aspidosperma quebracho-blanco* Schltdl. and *Bulnesia sarmientoi* Lorentz ex Griseb.

B. Available Ground Measurements

A summary of the average available data about the selected forest area is presented in Table I. This includes the distribution of diameter at breast height (dbh), which will be used in the simulations of Section IV. Additional ancillary information was extracted from an above-ground biomass (AGB) map, derived by MODIS [10]. This AGB was estimated using the Random Forest algorithm and the vegetation indices of MODIS. The resulting product was validated using independent biomass measurements. Using these data, a mean relative error of 3% and a maximum relative error of 15% were found [10]. The average dry biomass extracted from the AGB map is about 100 t/ha, for both Las Lomitas and Nueva Pompeya areas. Both local measurements [11] and a Food and Agriculture Organization (FAO) map [12] indicate the soil to be silty clay loam. In model simulations of Section IV, we have used FAO values, i.e., 25% sand and 35% clay.

In order to characterize the rain events, we have used the rainfall data collected in two meteorological stations: Las Lomitas and Nueva Pompeya. The locations are shown in Fig. 1. The accumulated precipitation was collected from 9:00 A.M. of a day until 9:00 A.M. of the next day, to record the total of the last 24 hours (www.corebe.org.ar). Rainfall data are shown in Figs. 2–5, concurrently with radiometric results. In January 2006, intense rainfalls occurred earlier in Las Lomitas (Julian day (JD) 21) and later in Nueva Pompeya (JD 23). In 2007, the events occurred in JD 339 and were intense in both stations. These two extreme events produced about 15% of the annual precipitation in one day.

C. Radiometric Data

Radiometric measurements were collected by the Advanced Microwave Scanning Radiometer (AMSR-E) of the Earth

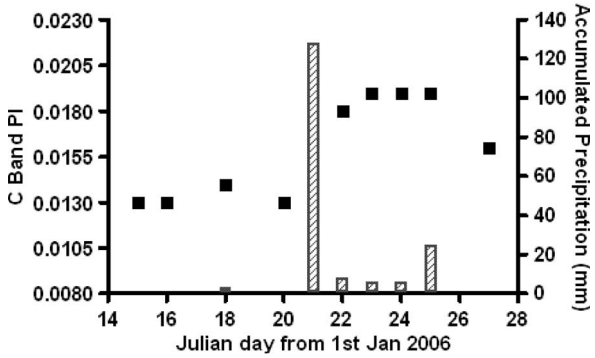

Fig. 2. Daily precipitation and C-band PI trend of Las Lomitas station for the days before and after the rain event that occurred on January 2006.

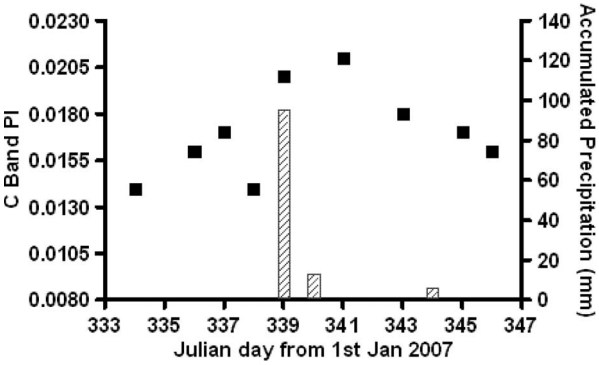

Fig. 3. Daily precipitation and C-band PI trend of Las Lomitas station for the days before and after the rain event that occurred on December 2007.

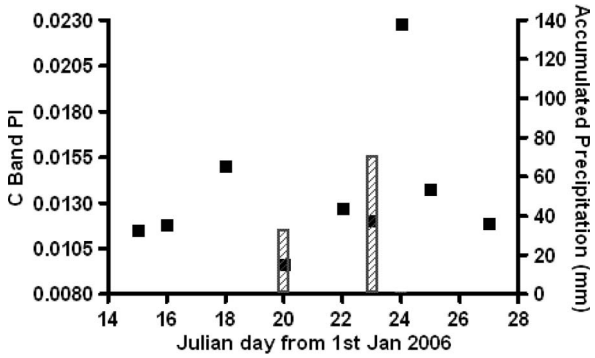

Fig. 4. Daily precipitation and C-band PI trend of Nueva Pompeya station for the days before and after the rain event that occurred on January 2006.

Observing System (EOS). The data have been downloaded from NASA site http://nsidc.org/ims-bin/pub/nph-ims.cgi/u885372. Details about the instrument are available in [1].

In particular, we considered C band signatures. In order to eliminate the dependence on surface temperature, we have used the PI [4], which is defined as:

$$\mathrm{PI} = \frac{T_{\mathrm{bv}} - T_{\mathrm{bh}}}{0.5(T_{\mathrm{bv}} + T_{\mathrm{bh}})} \tag{1}$$

where T_{bv} and T_{bh} are the brightness temperatures measured at vertical and horizontal polarization, respectively. At the higher frequencies, this index was used to monitor vegetation biomass [4]. However, it is also dependent on soil moisture, particularly at C band and lower frequencies [2].

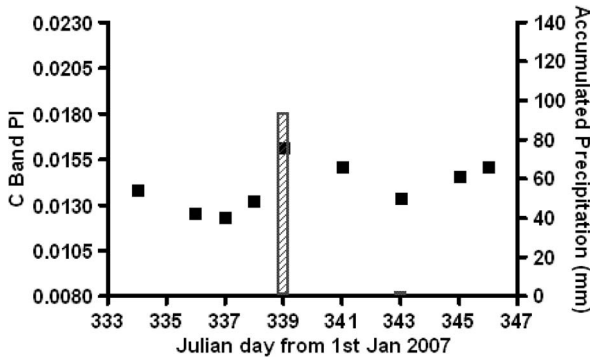

Fig. 5. Daily precipitation and C-band PI trend of Nueva Pompeya station for the days before and after the rain event that occurred on December 2007.

III. Radiometric Signatures of Rain Events

In order to analyze the temporal trend of PI, we have chosen an area of the size of an average C-band AMSR-E pixel near Las Lomitas which does not include the city (exact location: 24° 35′ 7.8″ S, 60° 28′ 2.7″ W; area: $\sim 45 \times 80$ km). In Figs. 2 and 3, the C Band PI trends of this area are shown for a period of approximately ten days both before and after the events. Rainfall data are also included in the figures. The temporal trend shows a rapid increase of PI on the day after the rain event, followed by a gradual decrease. After approximately days the PI returns to its initial value. A similar analysis was carried out for Nueva Pompeya station, and the results are shown in Fig. 4, for year 2006, and Fig. 5, for year 2007. In Fig. 4, the major increase is observed on Julian Day 24, following the rainfall of Julian Day 23. In the subsequent days, the PI decreases more rapidly than in the trends of Figs. 2 and 3. For the event of December 2007, the rainfall of Julian Day 339 produces a moderate effect on the PI of the same day. Since the descending orbit data were used and the precipitations are measured from 9:00 A.M. to 9:00 A.M. of the next day, a significant part of the rain event could have occurred earlier in the same day. After Julian Day 339, the PI decreases gradually.

In order to make a more quantitative evaluation of the effect, the average PI of the areas surrounding the two stations has been computed in several days characterized by drought and precipitation conditions, respectively. We defined a drought condition when there were more than 15 days without precipitation in the whole area. For the precipitation events, we took only samples collected one to three days following a rain event of at least 50 mm/day. Using these criteria, we selected samples for both drought and precipitation conditions for 2006 and 2007.

Relevant histograms are shown in Fig. 6 for the "drought" and the "precipitation" cases. The two histograms are significantly different (T-test: $p < 0.05$). The average value is 0.0151 (SD 0.0011) for the drought case and 0.0177 (SD 0.0023) for the precipitation case, while the maximum values are 0.019 and 0.025, respectively. The histogram of the precipitation case presents a higher variance.

In summary, these temporal and statistical analyses of PI during precipitation events indicate that there is a clear tendency of PI to increase after precipitation by an amount of about 0.004–0.005 units, which is moderate but detectable. The most convincing explanation is that the PI increases after rain

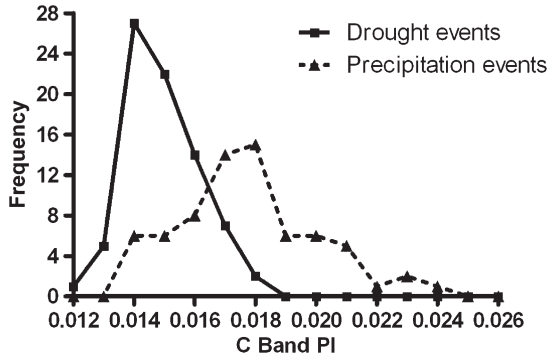

Fig. 6. C-band PI histogram for an ensemble of "drought" and "precipitation" days.

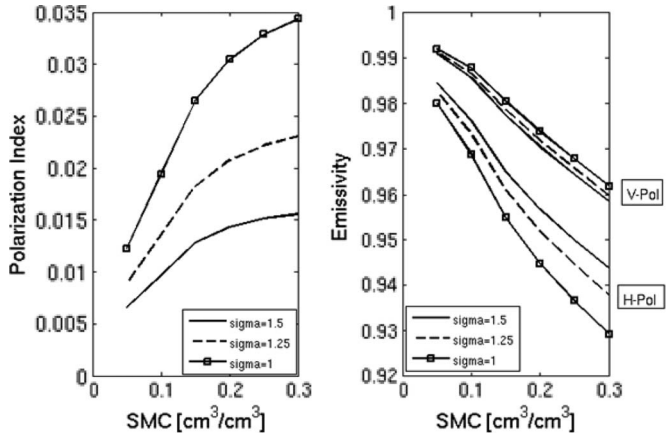

Fig. 7. Model simulation results. (Left) C-band PI as a function of volumetric SMC. (Right) Emissivity at (continuous lines) V and (dashed lines) H polarizations as a function of SMC.

due to changes in soil properties, particularly SMC, rather than raindrop interception or variation of canopy properties. In the literature, severe interception effects were found only in grass fields [13], [14], while were not so evident in forests [15]. Moreover, the effects of interception decreased rapidly with time, due to evaporation, and became negligible after 24 h [13]. In the climate of Chaco forest, the effect is even more rapid, since evaporation is higher than the one where the studies of [13] where carried out. On the contrary, Figs. 2–5 show that, after the rapid increase subsequent to rainfall, the changes of PI were generally slower, and compatible with the duration of soil drying processes at Chaco's evapotranspiration rates. Another possibility could be related to an increase of crown opacity due to wetting of branches and leaves, although there are no literature results showing evidence of this problem. In any case, interception and/or increase in canopy moisture should produce a decrease of PI, while an increase is observed after the rainfalls in our study area.

IV. Model Simulations

In order to interpret the observed trends of PI, the discrete forest model described in [16] has been used to simulate the variations of PI with soil moisture. The model has been run for a dry biomass $DB0 = 100$ t $\cdot$ ha^{-1} and the distribution of dbh given in Table I. The properties of woody material have been taken by http://www.inti.gov.ar/maderas/pdf/densidad_cientifico.pdf. It is important to note that most of the trees in the area belong to species characterized by heavy density wood, such as *Aspidosperma quebracho-blanco*, *Schinopsis lorentzii*, and *Bulnesia sarmientoi*. For *Aspidosperma quebracho-blanco*, the following densities (weights over fresh volume) are given: Fresh matter : $W = 1100$ kg/m^3; Dry matter : $W_D = 875$ kg/m^3.

We have used these values for the whole forest, since small differences are given for the other dominant species. According to well known formulas summarized in [17, Sec. II-B], we have: Water fraction by weight in wood : $VM = 0.204$; Dry matter density : $\rho_D = 1129$ kg/m^3. The Leaf Area Index is equal to 1.5, according to information available in ECOCLIMAP data base.

Using these data, the other canopy variables required by the model as input have been derived according to the procedure given in [17]. This procedure can be summarized into the following steps. For each class of dbh values, the total dry biomass and its subdivision into trunk, branch, and leaf contributions are derived using allometric equations, with coefficients obtained by averaging among values of broadleaf forests. A normalization factor is applied in order to impose the total dry biomass to be equal to the measured one. For each component, i.e., trunk, branch, and leaf, the dry biomass is converted into volume using the previously given values of ρ_D and VM. The distribution of trunk heights is related to the distribution of dbh. For branches, the maximum diameter is related to dbh and a Gaussian distribution of diameters is assumed. Branch orientation distribution is assumed to be uniform. For some critical parameters, the effects of variations with respect to average broadleaf values will be investigated later.

According to the literature [18], the average amount of litter in Chaco (most dried leaves and some small branches) is about 0.3 kg/m^2. This value has been used to simulate litter effect on soil emissivity. To this aim, we have adopted the layer model described in [17]. Information about soil roughness is not available at the scale of AMSR-E pixels. Simulations have been done under three assumptions about the standard deviation of surface height σ: 1, 1.25, and 1.5 cm. The correlation length l has been set equal to 5 cm. At C-band and higher frequencies, the surface emissivity is mostly dependent on the σ/l ratio. The cases considered by us correspond to σ/l equal to 0.2, 0.25, and 0.3, which are typically found in natural soils and adopted in parametric model simulations [19]. The volumetric soil moisture has been varied between 5% and 30%.

The left side of Fig. 7 shows the simulated trends of PI as a function of volumetric SMC. A direct comparison between measured and simulated values is not possible due to the unavailability of detailed information about soil moisture and roughness at the scale of AMSR-E signatures. However, simulations can provide sound explanations for the variations of PI described in Section III. As seen in the figure, the range of measured PI values (0.012–0.02) is within the range of simulated ones for the intermediate case of σ equal to 1.25 cm. Variations of σ have moderate effects in case of a dry soil, while they are important for higher values of SMC. In this context, it is possible that rainfall produces a smoothing of the soil surface besides an increase of SMC.

The right side of Fig. 7 shows the trends of emissivity as a function of SMC. Variations are moderate but can be detected. Model simulations indicate also that the transmissivity of the canopy at C-band is about 0.5 at horizontal polarization and 0.45 at vertical polarization. This confirms that an appreciable, although moderate, contribution of ground emission is present.

The results of Fig. 7 have been obtained using the input data indicated in Table I and also the procedure described in [17], in which some geometrical variables and allometric equations were derived by literature for broadleaf forests on average. We have investigated the effects of possible variations of some Chaco forest parameters with respect to values used in Fig. 7. In particular, we have considered the fraction of branch volume versus total volume and the ratio, and the maximum branch diameter, which can have an impact on the overall emissivity. The results (not shown here) indicate that changes of these variables influence the PI, but the general trends are similar to the ones of Fig. 7, and the interpretation of the effects described in Section III is still valid.

In summary, model simulations confirm that the increase of PI with SMC variations is moderate, but detectable, although C-band is considered and the forest is continuous. A first explanation of this result is related to the climatic conditions. The forest is located in a sunny region, the considered rain events occurred on summer and only minor rainfalls occurred in the antecedent days. This implies that the soil was dry before precipitation events. The diagrams of Fig. 7 indicate that the increases of SMC can be more easily detected if initial values are lower. Another explanation is related to the woody matter properties of the Chaco forest. Since the wood is hard, a biomass of 100 $\mathrm{t} \cdot \mathrm{ha}^{-1}$ corresponds to a volume of only 114 $\mathrm{m}^3 \cdot \mathrm{ha}^{-1}$, which produces a moderate attenuation. Therefore, the results of this study cannot be easily generalized to all forests. However, they are important, due to the extension and the environmental importance of the considered area and the existence of other dry forests around the world, which present similar forest characteristics.

V. Conclusion

In this letter, we have analyzed large rain events (70–120 mm/day) that occurred after dry periods in the Chaco Forest as seen by the C-band AMSR-E PI. In areas near Las Lomitas and Nueva Pompeya, we observed a significant increase of the PI after the rain events. Due to the temporal characteristics of the observed signatures, we associated these changes in PI to a change in soil moisture. A discrete model was run using measured forest data as input. Simulation outputs confirm that the variations of PI can be attributed to variations of soil properties and can predict an effect comparable with the measured one.

These results indicate that there is some sensitivity of AMSR-E C band signatures to variations of soil properties, at least in dry forests with moderate woody volume. The results cannot be directly exploited for operational purposes, but we expect to find a better sensitivity, even with less intense rain events, when long term multitemporal signatures, collected at L band, will be analyzed.

Acknowledgment

The authors would like to thank the members of Unidad de Manejo del Sistema Forestal Nacional, namely, G. Parmuchi and C. Montenegro, and the members of Comisión Regional del Río Bermejo (COREBE), namely, J. M. Bazán and R. C. Bignone, for their interaction and sharing of ideas and data.

References

[1] T. Kawanishi, T. Sezai, Y. Ito, K. Imaoka, T. Takeshima, Y. Ishido, A. Shibata, M. Miura, H. Inahata, and R. Spencer, "The Advanced Microwave Scanning Radiometer for the Earth Observing System (AMSR-E) NASDA's contribution to the EOS for global energy and water cycles studies," *IEEE Trans. Geosci. Remote Sens.*, vol. 41, no. 2, pp. 184–194, Feb. 2003.

[2] E. G. Njoku, T. L. Jackson, V. Lakshmi, T. Chan, and S. V. Nghiem, "Soil moisture retrieval from AMSR-E," *IEEE Trans. Geosci. Remote Sens.*, vol. 41, no. 2, pp. 215–229, Feb. 2003.

[3] R. Borchert, "Soil and stem water storage determine phenology and distribution of tropical dry forest trees," *Ecology*, vol. 75, no. 5, pp. 1437–1449, Jul. 1994.

[4] S. Paloscia and P. Pampaloni, "Microwave polarization index for monitoring vegetation growth," *IEEE Trans. Geosci. Remote Sens.*, vol. 26, no. 5, pp. 617–621, Sep. 1988.

[5] J. P. Grant, J.-P. Wigneron, A. A. Van de Griend, A. Kruszewsky, S. S. Søbjærg, and N. Skou, "A field experiment on microwave forest radiometry: L-band signal behaviour for varying conditions of surface wetness," *Remote Sens. Environ.*, vol. 109, no. 1, pp. 10–19, Jul. 2007.

[6] M. Guglielmetti, M. Schwank, C. Mätzler, C. Oberdörster, J. Vanderborght, and H. Flühler, "FOSMEX: Forest soil moisture experiments with microwave radiometry," *IEEE Trans. Geosci. Remote Sens.*, vol. 46, no. 3, pp. 727–735, Mar. 2008.

[7] E. Santi, S. Paloscia, P. Pampaloni, and S. Pettinato, "Ground-based microwave investigations of forest plots in Italy," *IEEE Trans. Geosci. Remote Sens.*, vol. 47, no. 9, pp. 3016–3025, Sep. 2009.

[8] UMSEF, "Mapa forestal provincia del Chaco," *Actualización Año 2007, Dirección de Bosques*, Secretaría de Ambiente y Desarrollo Sustentable, Ministerio de Salud, Buenos Aires, Argentina, 2008. 22 pp.

[9] UMSEF, *Monitoreo de la superficie de bosque nativo de Argentina*, 2007. [Online]. Available: http://www.ambiente.gov.ar/?idseccion=44

[10] N. Gasparri, "Efecto del cambio de uso de la tierra sobre la cobertura vegetal y la dinámica de biomasa del chaco semiárido Argentino," Ph.D. dissertation, Univ. Nacional Tucumán, Tucumán, Argentina, 2010.

[11] G. Cruzate, L. Gomez, M. J. Pizarro, P. Mercuri, and S. Banchero, "Suelos de la República Argentina (1:500.000)," SAGyP-INTA-Proyecto PNUD ARG/85/0192007.

[12] "FAO UNESCO soil map of the world," World Soil Resources, Rome, Italy, Rep. 60, 1988.

[13] K. Saleh, J. P. Wigneron, P. de Rosnay, J. C. Calvet, M. J. Escorihuela, Y. Kerr, and P. Waldteufel, "Impact of rain interception by vegetation and mulch on the L-band emission of natural grass," *Remote Sens. Environ.*, vol. 101, no. 1, pp. 127–139, Mar. 2006.

[14] K. Saleh, J.-P. Wigneron, P. Waldteufel, P. de Rosnay, M. Schwank, J.-C. Calvet, and Y. H. Kerr, "Estimates of surface soil moisture under grass covers using L-band radiometry," *Remote Sens. Environ.*, vol. 109, no. 1, pp. 42–53, Jul. 2007.

[15] J. P. Grant, K. Saleh, J. P. Wigneron, M. Guglielmetti, Y. H. Kerr, M. Schwank, N. Skou, and A. A. Van de Griend, "Calibration of the L-MEB model over a coniferous and a deciduous forest," *IEEE Trans. Geosci. Remote Sens.*, vol. 46, no. 3, pp. 808–818, Mar. 2008.

[16] P. Ferrazzoli and L. Guerriero, "Passive microwave remote sensing of forests: A model investigation," *IEEE Trans. Geosci. Remote Sens.*, vol. 34, no. 2, pp. 433–443, Mar. 1996.

[17] A. Della Vecchia, P. Ferrazzoli, L. Guerriero, R. Rahmoune, S. Paloscia, S. Pettinato, and E. Santi, "Modeling the multifrequency emission of broadleaf forests and their components," *IEEE Trans. Geosci. Remote Sens.*, vol. 48, no. 1, pp. 260–272, Jan. 2010.

[18] A. Abril and E. H. Bucher, "Overgrazing and soil carbon dynamics in the western Chaco of Argentina," *Appl. Soil Ecology*, vol. 16, no. 3, pp. 243–249, Mar. 2001.

[19] F. T. Ulaby, R. K. Moore, and A. K. Fung, "Microwave remote sensing, active and passive," in *From Theory to Applications*, vol. 3. Dedham, MA: Artech House, 1986.